



# Quantitative Analysis on Ex Vivo Nonlinear Microscopy Images of Basal Cell Carcinoma Samples in Comparison to Healthy Skin

Norbert Kiss<sup>1,2</sup> · Dóra Haluszka<sup>1,2</sup> · Kende Lőrincz<sup>2</sup> · Nóra Gyöngyösi<sup>2</sup> · Szabolcs Bozsányi<sup>2</sup> · András Bánvölgyi<sup>2</sup> · Róbert Szipócs<sup>1,3</sup> · Norbert Wikonkál<sup>2</sup>

Received: 22 December 2017 / Accepted: 19 June 2018 / Published online: 6 July 2018  
© Arányi Lajos Foundation 2018

## Abstract

Basal cell carcinoma (BCC) is the most frequent malignant neoplasm in the Caucasian population. There are several therapeutic options for BCC, but surgical excision is considered gold standard treatment. As BCCs often have poorly defined borders, the clinical assessment of the tumor margins can be challenging. Therefore, there is an increasing demand for efficient *in vivo* imaging techniques for the evaluation of tumor borders prior to and during surgeries. In the near future, nonlinear microscopy techniques might meet this demand. We measured the two-photon excitation fluorescence (TPEF) signal of nicotinamide adenine dinucleotide hydride (NADH) and elastin and second harmonic generation (SHG) signal of collagen on 10 *ex vivo* healthy control and BCC skin samples and compared the images by different quantitative image analysis methods. These included integrated optical density (IOD) measurements on TPEF and SHG images and application of fast Fourier transform (FFT), CT-FIRE and CurveAlign algorithms on SHG images to evaluate the collagen structure. In the BCC samples, we found significantly lower IOD of both the TPEF and SHG signals and higher collagen orientation index utilizing FFT. CT-FIRE algorithm revealed increased collagen fiber length and decreased fiber angle while CurveAlign detected higher fiber alignment of collagen fibers in BCC. These results are in line with previous findings which describe pronounced changes in the collagen structure of BCC. In the future, these novel image analysis methods could be integrated in handheld nonlinear microscope systems, for sensitive and specific identification of BCC.

**Keywords** Basal cell carcinoma · Nonlinear microscopy · Second-harmonic generation · Collagen structure · Quantitative analysis

## Introduction

Basal cell carcinoma (BCC) is the most frequent malignant neoplasm in the Caucasian population [1]. The incidence of BCC varies greatly worldwide, with the highest rates in Australia (>1000/100000 person-years) and the lowest rates in parts of Africa (<1/100000 person-years) [2]. The most important risk factors for BCC include fair skin phenotype

and excessive occasional sun exposure [3]. Although the metastatic rate of BCC is very low, it can lead to significant tissue destruction by local invasion to result in major cosmetic damage and inoperable propagation, thus early diagnosis of BCC is crucial [4].

There are several therapeutic options for BCC, including cryo-, photodynamic- and radiotherapy [5], but surgical excision is considered gold standard. Among surgical techniques, Mohs micrographic surgery (MMS) provides the lowest rate of tumor recurrence with the smallest resected area by utilizing repeated microscopic examinations of frozen sections of the tumor margins during surgery. However, MMS is a time-consuming technique that also requires special expertise. As BCCs often have poorly defined borders, without utilizing MMS, the clinical assessment of the tumor margins can be challenging [6]. Therefore, there is an increasing demand for efficient *in vivo* imaging techniques for the evaluation of the tumor borders of BCC prior to and during surgeries. In the near future, nonlinear microscopy techniques might meet this demand [7].

✉ Róbert Szipócs  
r.szipocs@szipocs.com

<sup>1</sup> Wigner RCP, Institute for Solid State Physics and Optics, P.O. Box 49, Budapest H-1525, Hungary

<sup>2</sup> Department of Dermatology, Venereology and Dermatocology, Semmelweis University, Budapest, Hungary

<sup>3</sup> R&D Ultrafast Lasers Ltd, P.O. Box 622, Budapest H-1539, Hungary

Nonlinear microscopy utilizes the nonlinear interactions of light, when light-induced dielectric polarization depends nonlinearly on the electric field of light [8]. In the last 20 years, various nonlinear optical techniques, including two photon excitation fluorescence (TPEF) and second harmonic generation (SHG) microscopy have been developed as novel imaging approaches [7]. TPEF microscopy enables high-resolution detection of endogenous fluorophores, such as elastin, nicotinamide adenine dinucleotide hydride (NADH), melanin and keratin. SHG signals are generated during the polarization of non-centrosymmetric molecules with high structural regularity, such as myosin, microtubules and collagen fibers [9]. The combination of SHG and TPEF is capable of visualizing the morphology of both the extracellular matrix and cells of the skin [6]. Nonlinear microscopy techniques have also been applied for the imaging of BCC [9–11].

Recently, several ways of quantitative image analyses have been utilized to evaluate the collagen structure in nonlinear microscopy images of different conditions, including skin aging and different types of cancers [12–15]. To date, these techniques have not been employed for the assessment of BCC. We carried out nonlinear microscopy measurements on *ex vivo* healthy control and BCC skin samples and compared the images by different quantitative image analysis methods. We set out to evaluate the applicability of various parameters provided by these methods in the detection of BCC.

## Materials and Methods

### Sample Preparation

We collected 10 nodular-type BCC and healthy skin samples at our department after surgical excision. Samples were kept in phosphate buffered saline and chilled on ice. To avoid tissue degradation, nonlinear microscopy measurements were performed within 1–3 h after the excision. Prior to measurements, we placed the unfixed samples on slides and applied coverslips. Following the imaging, we fixed the samples in formalin and embedded in paraffin. The diagnosis of BCC was confirmed by standard histopathologic examination of all samples.

### Nonlinear Microscopic Imaging Setup

We captured nonlinear microscopy images by a commercial Axio Examiner LSM 7 MP laser scanning two-photon microscope (Carl Zeiss AG, Jena, Germany), with custom-modified detection optics for TPEF and SHG imaging. A tunable, femtosecond pulse Ti-sapphire laser (*FemtoRose 100TUN NoTouch*, R&D Ultrafast Lasers Ltd., Budapest, Hungary) was utilized, operated at 796 nm center excitation wavelength, which delivered nearly transform limited,  $\tau_{FWHM} \sim 190$  fs pulses at a repetition rate of  $\sim 76$  MHz. The average power

of the laser beam measured at the sample surface was typically  $\sim 20$  mW. A 460/50 nm band-pass emission filter was employed to separate TPEF signal and a 405/20 nm band-pass emission filter was used to isolate SHG signal. We utilized computer controlled positioning of the objective along the z-axis for the acquisition of images (z-stack images) of various tissue depths. To focus the laser beams, a 20 $\times$  water immersion objective (W-Plan – APOCHROMAT 20 $\times$ /1,0 DIC (UV) VIS-IR, Carl Zeiss AG, Germany), was employed, with an imaging area of approximately  $0.42 \times 0.42$  mm<sup>2</sup>. From each sample, we acquired three z-stack images. The imaging setup is described in more detail in Ref. [16].

### Integrated Optical Density Measurements

TPEF signal of NADH and elastin and SHG signal of unimpaired collagen was quantified by converting the measured intensities to integrated optical density (IOD) by ImageJ software (NIH, USA) [17].

### Fast Fourier Transformation

Fast Fourier Transformation (FFT) is a computational device which facilitates signal analysis. It is a widely used method to measure the degree of organization and symmetry of collagen fibers [15, 18, 19]. We used FFT to convert the original data images of SHG and TPF signals from “real” space into mathematically defined “frequency” space. The output of the FFT is an image in which the distribution pattern of pixels reflects the degree of fiber alignment in the original image [20]. We converted the output images to power plots for more accurate analysis [21]. As the eccentricity of the power plots describes the arrangement of the collagen fibers, an ellipse was fitted to each power plot and we calculated collagen orientation index (COI) by  $COI = [1 - (\text{short axis}/\text{long axis})]$ . A circular power plot with a COI close to 0 reflects a normal skin sample where collagen shows an isotropic behavior, while an elongated power plot with a COI close to 1 indicates parallelly-oriented fibers [12, 15]. Collagen bundle packing (CBP) represents periodicity in collagen, and was expressed as  $CPB = 512 \cdot (1/h)$ , where h is the distance between the centers of gravity of two first-order maxima of FFT plots [12]. FFT processing and image analysis were performed using ImageJ.

### CT-FIRE and CurveAlign

CT-FIRE and CurveAlign (LOCI, USA) are curvelet-based frameworks which are designed to provide information about the collagen structure [14]. CT-FIRE combines the advantages of the filter based and fiber tracking methods to extract and analyze collagen fibers from SHG images. The curvelet transform (CT) is a fast discrete preprocessing mechanism, which de-noises the image. A threshold is used to form a binary

image, which is followed by the application of a distance transform. After creating nucleation points from the smoothed images, branches are formed based on the fiber trajectory [13]. Fiber tracking (FIRE) is an algorithm to extract individual fibers from fiber networks. With its built-in thresholding and element superposition pre-and post-processing tools, CT-FIRE is capable of measuring individual fiber metrics [14].

CurveAlign targets to detect all fiber angles in a region of interest and to perform bulk assessment of collagen features. It compares density and alignment of fibers with boundaries and fibers to each other [22]. CT-FIRE (v1.3) and CurveAlign (v4.0) were run on the raw SHG images to calculate the following parameters: fiber length, angle, width and straightness (CT-FIRE); fiber alignment and orientation (CurveAlign).

## Statistical Analysis

We performed the statistical analysis using GraphPad Prism v6.0 (GraphPad Software Inc., USA). Data were analyzed using Student's *t*-test after the normal distribution was confirmed by F test. Results were considered significant if  $p < 0.05$ .

## Results

The IOD values of the SHG and TPF images of the BCC samples were significantly lower than images of normal skin

(Fig. 1). FFT transformed SHG images of BCC displayed significantly higher COI than controls, indicating that in the BCC samples the collagen fibers are less randomly arranged, while there was no difference in the CBP value (Fig. 2). CT-FIRE algorithm revealed increased collagen fiber length and decreased fiber angle in the BCC samples compared to controls (Fig. 3). Collagen width and straightness values were similar in the BCC and control samples. CurveAlign software detected significantly higher fiber alignment of collagen fibers in BCC samples than healthy skin (Fig. 4). Collagen fiber orientation values showed high standard deviation and no significant difference was detected between BCC and control samples in this parameter.

## Discussion

To date, various diagnostic imaging tools have been applied for the non-invasive assessment of different skin lesions, including BCC. Johan Christophorus Kolhaus was the first to attempt skin-surface microscopy in 1663 [23], while dermatoscope was developed in 1958. Dermatoscopes are epiluminescent manual microscopes with a typical magnification of  $10\times$  [24, 25]. Dermoscopy is cost-effective and its use increases the diagnostic accuracy by 5-30% over visual inspection [26]. On the other hand, established dermoscopic criteria are often absent in superficial BCC, and the magnification is low for precise

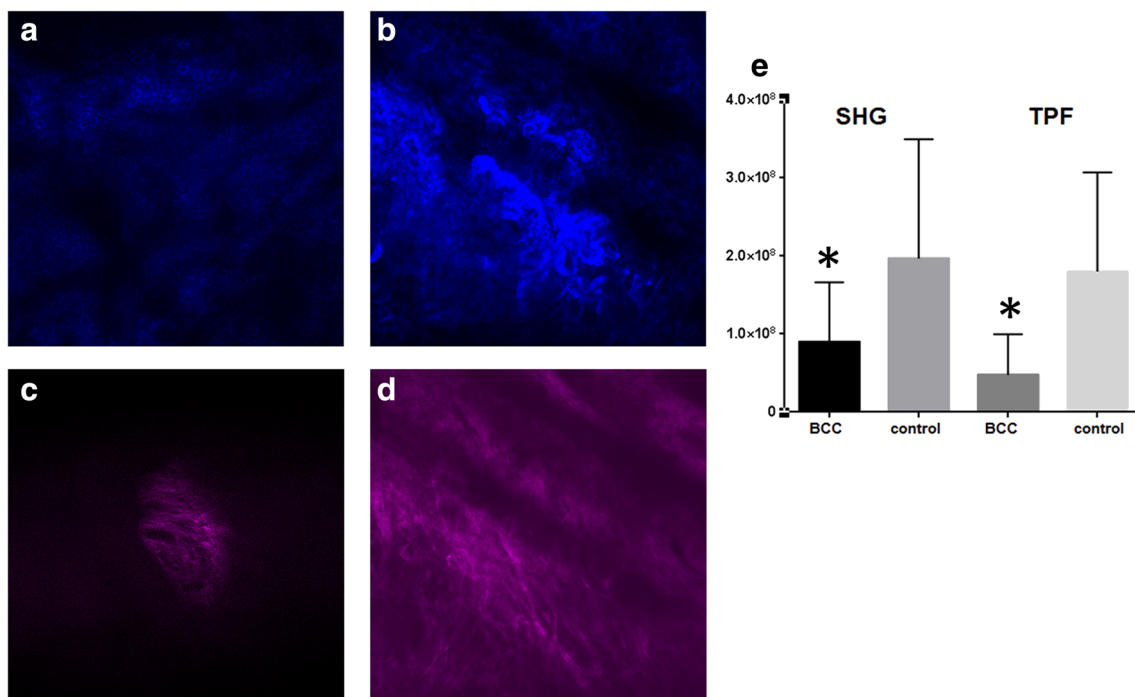


**Fig. 1** Two-photon absorption fluorescence (TPF) and second harmonic generation (SHG) images of basal cell carcinoma (BCC) and healthy skin. **a, b:** TPF; **c, d:** SHG; **a, c:** BCC; **b, d:** control skin; **e:** Integrated optical

density of BCC and control skin. Error bars represent standard deviation,  $*p < 0.05$ . Size of the images is  $420 \times 420 \mu\text{m}^2$

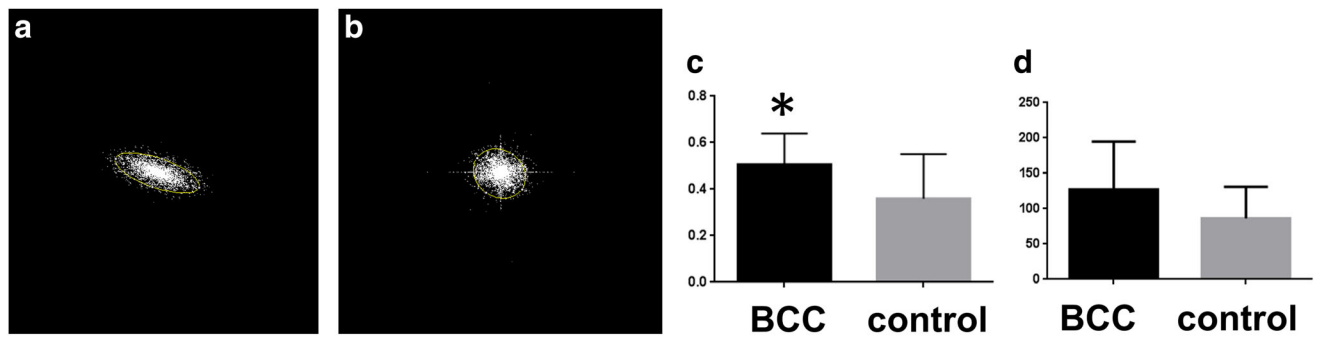


**Fig. 2** **a, b** panels: Power plots of fast Fourier transformed second harmonic generation (SHG) images; **a**: basal cell carcinoma (BCC), **b**: control skin. **c**: collagen orientation index; **d**: collagen bundle packing. Error bars represent standard deviation, \* $p < 0.05$

assessment of tumor margins [6]. Furthermore, automated quantitative image analysis of digital dermoscopy images has been only applied for the assessment of melanocytic lesions [27]. In 1979 Alexander and Miller were the first to employ high frequency ultrasound (HFUS) for the examination of the skin [28]. HFUS can be used to examine the depth of BCC, but it only provides a low resolution image [29]. Recently, quantitative parameters based on HFUS were also introduced for the identification of BCC [30]. Optical coherence tomography (OCT) is used in ophthalmology since 1986 [31], and it proved to be also suitable for the visualization of altered skin architecture in BCC [32]. In 2016, an automated procedure to detect BCC based on the analysis of quantitative features of OCT images utilizing machine learning was reported, although its major disadvantage is long computation time [33]. The

principles of reflectance confocal microscopy (RCM) have been described in 1957, but it appeared in the clinical practice only in the last two decades. [34]. RCM provides higher resolution, but lower penetration depth compared to OCT and HFUS [35]. In the last decade, RCM was also employed to aid the diagnosis of BCC, but it lacks standardized criteria and data from experimental studies are found to be hard to reproduce in real-life settings [36].

While in recent years several papers have been published on quantitative analysis of BCC based on various non-invasive imaging modalities including digital dermoscopy, HFUS and OCT, such analyses were not performed on non-linear microscopy images. At the same time, changes in the collagen structure in SHG images have been assessed for the detection of different types of cancers and skin diseases. For

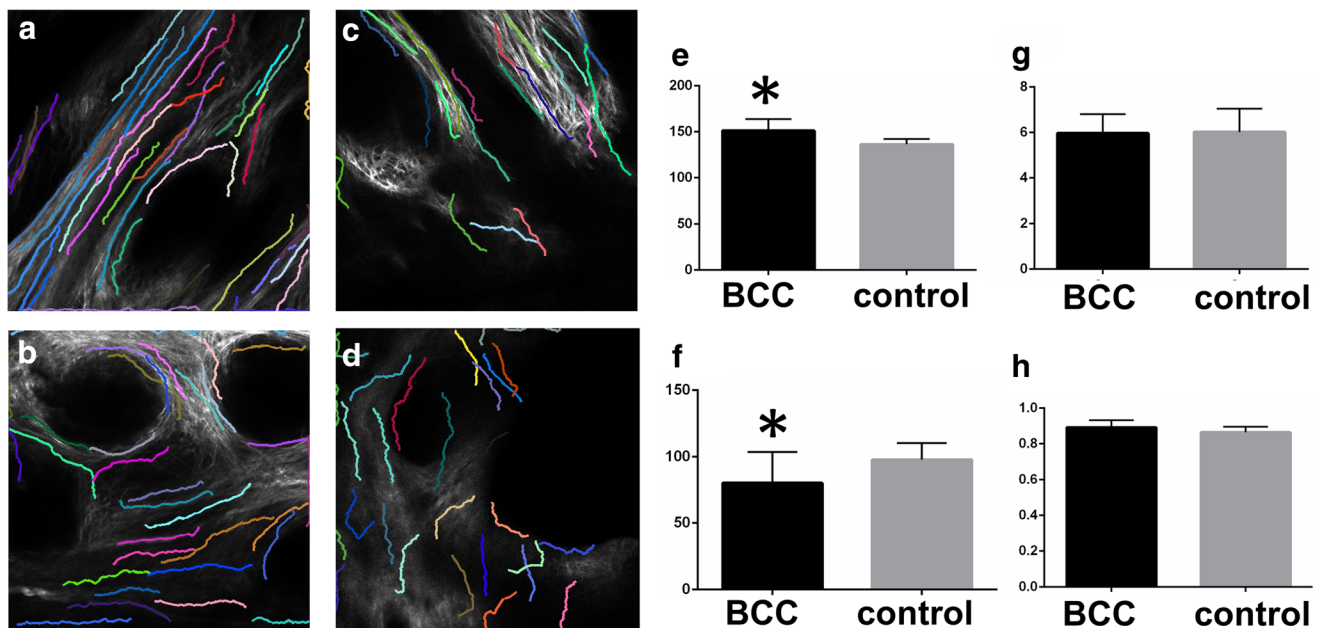


**Fig. 3** Output images and data of CT FIRE algorithm performed on second harmonic generation (SHG) images. **a, b**: basal cell carcinoma (BCC); **c, d**: control skin; **E-H**: results of CT FIRE algorithm,

parameters of collagen fibers: **e**: length, **f**: angle, **g**: width, **h**: straightness. Error bars represent standard deviation, \* $p < 0.05$ . Size of the images is  $420 \times 420 \mu\text{m}^2$

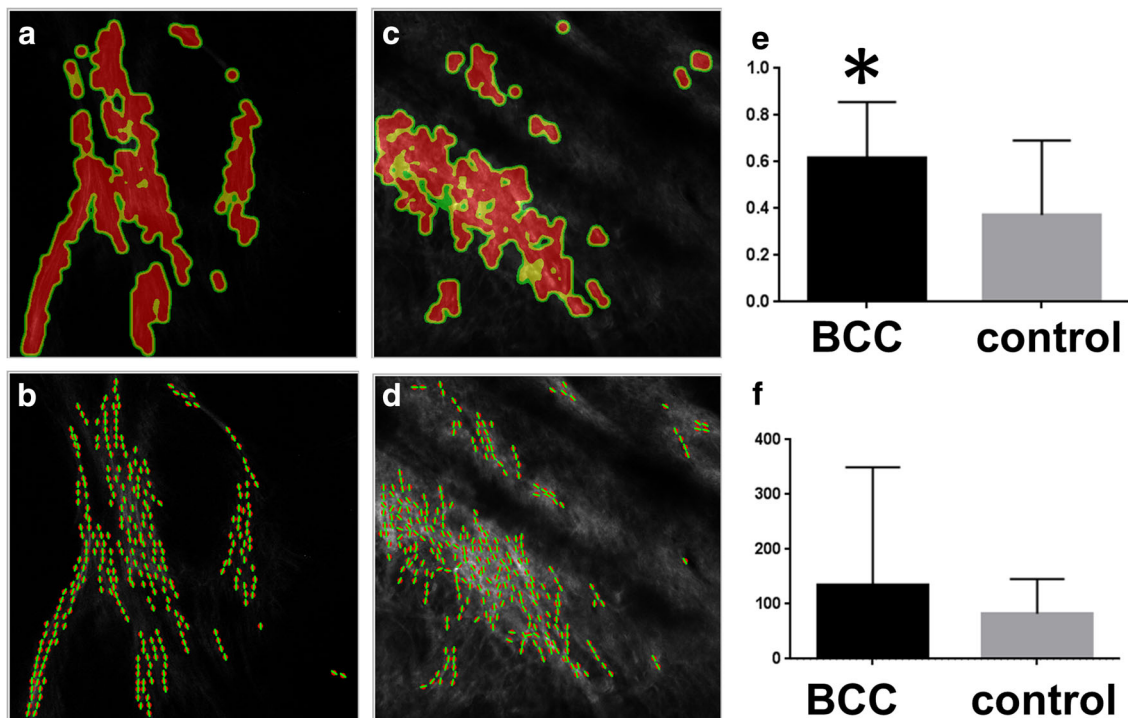


**Fig. 4** Output images and data of CurveAlign algorithm performed on second harmonic generation (SHG) images. **a, b:** basal cell carcinoma (BCC); **c, d:** control skin; **a, c:** heatmap output image; **b, d:** overlaid

output image; **e:** collagen fiber alignment **f:** collagen fiber orientation. Error bars represent standard deviation,  $*p < 0.05$ . Size of the images is  $420 \times 420 \mu\text{m}^2$

the detection of BCC, among quantitative parameters only SHG and TPEF intensities were evaluated in previous studies [37]. Although we detected significantly lower IOD of TPEF signals of NADH and elastin and SHG signal of collagen in the BCC samples, we regard IOD a less reliable parameter as it depends on many external factors including the excitation intensity, the depth of the imaging and thickness of the epidermis. As the quantitative assessment approaches of the morphology of collagen fibers in BCC and healthy skin samples are not influenced by these factors, these could be promising methods. While our analysis of FFT transformed images revealed higher COI in the BCC samples, we learnt from mouse studies that COI can also be elevated due to collagen rearrangement in intrinsic skin aging, wounded skin and scleroderma [12, 15, 21]. Similarly to our findings, Drifka et al. detected significantly higher collagen fiber length and decreased fiber angle by CT-FIRE algorithm in *ex vivo* pancreatic cancer samples, whereas they also found increased collagen width and straightness [14]. The increased orientation of collagen fibers, which we measured in BCC samples by employing CurveAlign software, have been reported to play a critical role in the local invasion of breast cancer [38]. Thus, the assessment of collagen fiber orientation could be a potential tool to identify local invasion capacity. In the end, our results are in line with previous findings which describe pronounced changes in the arrangement of collagen fibers in BCC [9, 37, 39].

Additionally, open source machine learning environments, such as Weka (University of Waikato, New Zealand) and PRTools (Delft University of Technology, Netherlands) could be utilized to improve these algorithms specifically for the detection of BCC. Quantitative image analysis, including a custom combination of FFT, CT-FIRE and CurveAlign methods could be integrated in handheld nonlinear microscope systems [40], for identification and detection of tumor borders of BCC in the future. Following further research, these imaging systems could be also applied for the diagnostics and therapy follow-up of solar keratoses and keratoacanthomas among other skin lesions. Further studies may assess the sensitivity and specificity of these methods compared with other non-invasive diagnostic techniques.

**Acknowledgements** We acknowledge the work of our dermatopathology team, Enikő Kuroli and Judit Hársing for reading the histological sections.

### Compliance with Ethical Standards

**Conflict of Interest** The authors declare that they have no conflict of interest.

**Ethical Approval** All procedures performed in studies involving human participants were in accordance with the ethical standards of the institutional and/or national research committee and with the 1964 Helsinki declaration and its later amendments or comparable ethical standards. All applicable international, national, and/or institutional guidelines for the care and use of animals were followed.

## References

1. Goldenberg G, Karagiannis T, Palmer JB, Lotya J, O'Neill C, Kisa R, Herrera V, Siegel DM (2016) Incidence and prevalence of basal cell carcinoma (BCC) and locally advanced BCC (LABCC) in a large commercially insured population in the United States: a retrospective cohort study. *J Am Acad Dermatol* 75(5):957–966 e952. <https://doi.org/10.1016/j.jaad.2016.06.020>
2. Lomas A, Leonardi-Bee J, Bath-Hextall F (2012) A systematic review of worldwide incidence of nonmelanoma skin cancer. *Br J Dermatol* 166(5):1069–1080
3. Zanetti R, Rosso S, Martinez C, Nieto A, Miranda A, Mercier M, Loria D, Østerlind A, Greinert R, Navarro C (2006) Comparison of risk patterns in carcinoma and melanoma of the skin in men: a multi-centre case–case–control study. *Br J Cancer* 94:743–751
4. Crowson A (2006) Basal cell carcinoma: biology, morphology and clinical implications. *Mod Pathol* 19:S127–S147
5. Gandhi SA, Kamp J (2015) Skin cancer epidemiology, detection, and management. *Med Clin North Am* 99(6):1323–1335
6. Seidenari S, Arginelli F, Bassoli S, Cautela J, Cesinaro AM, Guanti M, Guardoli D, Magnoni C, Manfredini M, Ponti G (2013) Diagnosis of BCC by multiphoton laser tomography. *Skin Res Technol* 19(1)
7. Cicchi R, Kapsokalyvas D, Pavone FS (2014) Clinical nonlinear laser imaging of human skin: a review. *Biomed Res Int* 2014:903589. <https://doi.org/10.1155/2014/903589>
8. Tong L, Cheng J-X (2011) Label-free imaging through nonlinear optical signals. *Mater Today* 14(6):264–273. [https://doi.org/10.1016/S1369-7021\(11\)70141-9](https://doi.org/10.1016/S1369-7021(11)70141-9)
9. Balu M, Zachary CB, Harris RM, Krasieva TB, Konig K, Tromberg BJ, Kelly KM (2015) In vivo multiphoton microscopy of basal cell carcinoma. *JAMA Dermatol* 151(10):1068–1074. <https://doi.org/10.1001/jamadermatol.2015.0453>
10. Seidenari S, Arginelli F, Bassoli S, Cautela J, Cesinaro AM, Guanti M, Guardoli D, Magnoni C, Manfredini M, Ponti G, Konig K (2013) Diagnosis of BCC by multiphoton laser tomography. *Skin Res Technol* 19(1):e297–e304. <https://doi.org/10.1111/j.1600-0846.2012.00643.x>
11. Kiss N, Krolopp A, Lorincz K, Banvolgyi A, Szipocs R, Wikonkal N (2017) Stain-free histopathology of basal cell carcinoma by dual vibration resonance frequency CARS microscopy. *Pathol Oncol Res* <https://doi.org/10.1007/s12253-017-0356-6>
12. Wu S, Li H, Yang H, Zhang X, Li Z, Xu S (2011) Quantitative analysis on collagen morphology in aging skin based on multiphoton microscopy. *J Biomed Opt* 16(4):040502. <https://doi.org/10.1117/1.3565439>
13. Bredfeldt JS, Liu Y, Pehlke CA, Conklin MW, Szulcowski JM, Inman DR, Keely PJ, Nowak RD, Mackie TR, Eliceiri KW (2014) Computational segmentation of collagen fibers from second-harmonic generation images of breast cancer. *J Biomed Opt* 19(1)
14. Drifka CR, Loeffler AG, Mathewson K, Mehta G, Keikhosravi A, Liu Y, Lemancik S, Ricke WA, Weber SM, Kao WJ (2016) Comparison of picosirius red staining with second harmonic generation imaging for the quantification of clinically relevant collagen fiber features in histopathology samples. *J Histochem Cytochem* 64(9):519–529
15. Li J, Bower AJ, Vainstein V, Gluzman-Poltorak Z, Chaney EJ, Marjanovic M, Basile LA, Boppart SA (2015) Effect of recombinant interleukin-12 on murine skin regeneration and cell dynamics using in vivo multimodal microscopy. *Biomed Opt Express* 6(11):4277–4287. <https://doi.org/10.1364/boe.6.004277>
16. Haluszka D, Lorincz K, Kiss N, Szipocs R, Kuroli E, Gyongyosi N, Wikonkal NM (2016) Diet-induced obesity skin changes monitored by in vivo SHG and ex vivo CARS microscopy. *Biomed Opt Express* 7(11):4480–4489. <https://doi.org/10.1364/BOE.7.004480>
17. Lorincz K, Haluszka D, Kiss N, Gyongyosi N, Banvolgyi A, Szipocs R, Wikonkal NM (2017) Voluntary exercise improves murine dermal connective tissue status in high-fat diet-induced obesity. *Arch Dermatol Res* 309(3):209–215. <https://doi.org/10.1007/s00403-017-1715-6>
18. Cicchi R, Kapsokalyvas D, De Giorgi V, Maio V, Van Wiechen A, Massi D, Lotti T, Pavone FS (2010) Scoring of collagen organization in healthy and diseased human dermis by multiphoton microscopy. *J Biophotonics* 3(1-2):34–43
19. James W, Cooley P, Peter DW (1967) Historical notes on the fast Fourier transform. *Proc IEEE* 55(10):1675
20. Ayres C, Bowlin GL, Henderson SC, Taylor L, Shultz J, Alexander J, Telemeco TA, Simpson DG (2006) Modulation of anisotropy in electrospun tissue-engineering scaffolds: analysis of fiber alignment by the fast Fourier transform. *Biomaterials* 27(32):5524–5534
21. Lu K, Chen J, Zhuo S, Zheng L, Jiang X, Zhu X, Zhao J (2009) Multiphoton laser scanning microscopy of localized scleroderma. *Skin Res Technol* 15(4):489–495
22. Walsh AJ, Cook RS, Lee JH, Arteaga CL, Skala MC (2015) Collagen density and alignment in responsive and resistant trastuzumab-treated breast cancer xenografts. *J Biomed Opt* 20(2)
23. Gilje O, O'Leary PA, Baldes EJ (1953) Capillary microscopic examination in skin diseases. *AMA Arch Derm Syphilol* 68(2):136–147
24. Goldman L (1958) A simple portable skin microscope for surface microscopy. *AMA Arch Derm* 78(2):246–247. <https://doi.org/10.1001/archderm.1958.01560080106017>
25. Argenziano G, Soyer HP, Chimenti S, Talamini R, Corona R, Sera F, Binder M, Cerroni L, De Rosa G, Ferrara G (2003) Dermoscopy of pigmented skin lesions: results of a consensus meeting via the internet. *J Am Acad Dermatol* 48(5):679–693
26. Braun RP, Rabinovitz HS, Oliviero M, Kopf AW, Saurat J-H (2005) Dermoscopy of pigmented skin lesions. *J Am Acad Dermatol* 52(1):109–121. <https://doi.org/10.1016/j.jaad.2001.11.001>
27. Anagnostopoulos CN, Vergados DD, Anagnostopoulos I, Mintzias P (2014) Total dermoscopy score calculation using quantitative measurements in digital dermoscopy. *Conf Proc IEEE Eng Med Biol Soc* 2014:6744–6747. <https://doi.org/10.1109/embc.2014.6945176>
28. Alexander H, Miller DL (1979) Determining skin thickness with pulsed ultra sound. *J Invest Dermatol* 72(1):17–19
29. Lockwood G, Turnbull D, Christopher D, Foster FS (1996) Beyond 30 MHz [applications of high-frequency ultrasound imaging]. *IEEE Eng Med Biol Mag* 15(6):60–71
30. Piotrkowska-Wroblewska H, Litniewski J, Szymanska E, Nowicki A (2015) Quantitative sonography of basal cell carcinoma. *Ultrasound Med Biol* 41(3):748–759. <https://doi.org/10.1016/j.ultrasmedbio.2014.11.016>
31. Fercher A, Roth E (1986) Ophthalmic laser interferometry. In: *Optical instrumentation for biomedical laser applications*. International Society for Optics and Photonics, pp 48–52
32. Gambichler T, Orlikov A, Vasa R, Moussa G, Hoffmann K, Stücker M, Altmeyer P, Bechara FG (2007) In vivo optical coherence tomography of basal cell carcinoma. *J Dermatol Sci* 45(3):167–173. <https://doi.org/10.1016/j.jdermsci.2006.11.012>
33. Marvdashti T, Duan L, Aasi SZ, Tang JY, Ellerbee Bowden AK (2016) Classification of basal cell carcinoma in human skin using machine learning and quantitative features captured by polarization sensitive optical coherence tomography. *Biomed Opt Express* 7(9):3721–3735
34. Calzavara-Pinton P, Longo C, Venturini M, Sala R, Pellacani G (2008) Reflectance confocal microscopy for in vivo skin imaging. *Photochem Photobiol* 84(6):1421–1430. <https://doi.org/10.1111/j.1751-1097.2008.00443.x>

35. Gambichler T, Jaedicke V, Terras S (2011) Optical coherence tomography in dermatology: technical and clinical aspects. *Arch Dermatol Res* 303(7)
36. Kadouch DJ, Schram ME, Leeflang MM, Limpens J, Spuls PI, de Rie MA (2015) In vivo confocal microscopy of basal cell carcinoma: a systematic review of diagnostic accuracy. *J Eur Acad Dermatol Venereol* 29(10):1890–1897. <https://doi.org/10.1111/jdv.13224>
37. Lin SJ, Jee SH, Kuo CJ, Wu RJ, Lin WC, Chen JS, Liao YH, Hsu CJ, Tsai TF, Chen YF, Dong CY (2006) Discrimination of basal cell carcinoma from normal dermal stroma by quantitative multiphoton imaging. *Opt Lett* 31(18):2756–2758
38. Provenzano PP, Eliceiri KW, Campbell JM, Inman DR, White JG, Keely PJ (2006) Collagen reorganization at the tumor-stromal interface facilitates local invasion. *BMC Med* 4(1):38. <https://doi.org/10.1186/1741-7015-4-38>
39. Short MA, Lui H, McLean D, Zeng H, Alajlan A, Chen XK (2006) Changes in nuclei and peritumoral collagen within nodular basal cell carcinomas via confocal micro-Raman spectroscopy. *J Biomed Opt* 11(3):34004. <https://doi.org/10.1117/1.2209549>
40. Krolopp A, Csakanyi A, Haluszka D, Csati D, Vass L, Kolonics A, Wikonkal N, Szipoos R (2016) Handheld nonlinear microscope system comprising a 2 MHz repetition rate, mode-locked Yb-fiber laser for in vivo biomedical imaging. *Biomed Opt Express* 7(9): 3531–3542. <https://doi.org/10.1364/boe.7.003531>